Service-based Reliability Analysis of Integrated Electricity-heat Systems Considering Thermal Dynamics

Xunhu Yin, Minglei Bao, Yi Ding, Chengjin Ye, Peng Wang, and Lalit Goel

***Abstract*—The essential task of integrated electricity-heat systems (IEHSs) is to provide customers with reliable electric and heating services. From the perspective of customers, it is reasonable to analyze the reliabilities of IEHSs based on the ability to provide energy services with a reasonable assurance of continuity and quality, which are termed as service-based reliabilities. Due to the thermal inertia existing in IEHSs, the heating service performances can present slow dynamic characteristics, which has a great impact on the service satisfaction of customers. The neglect of such thermal dynamics will bring about inaccurate service-based reliability measurement, which can lead to the inefficient dispatch decisions of system operators. Therefore, it is necessary to provide a tool which can analyze the service-based reliabilities of IEHSs considering the impacts of thermal dynamics. This paper firstly models the energy service performance of IEHSs in contingency states. Specifically, the nodal energy supplies are obtained from the optimal power and heat flow model under both variable hydraulic and thermal conditions, in which the transmission-side thermal dynamics are formulated. On this basis, the energy service performances for customers are further determined with the formulation of demand-side thermal dynamics. Moreover, a service-based reliability analysis framework for the IEHSs is proposed utilizing the time-sequential Monte Carlo simulation (TSMCS) technique with the embedded decomposition algorithm. Furthermore, the indices for quantifying service-based reliabilities are defined based on the traditional reliability indices, where dynamic service performances and service satisfactions of customers are both considered. Numerical simulations are carried out with a test system to validate the effectiveness of the proposed framework.**

***Index Terms*—Energy service, integrated electricity-heat system, reliability, thermal dynamics.**

Manuscript received: August 10, 2022; revised: December 28, 2022; accepted: March 1, 2023. Date of CrossCheck: March 1, 2023. Date of online publication: April 5, 2023.

This work was supported by the Science and Technology Project of State Grid Corporation of China (No. 5108-202218280A-2-448-XG).

X. Yin, M. Bao (corresponding author), Y. Ding, and C. Ye are with the College of Electrical Engineering, Zhejiang University, Hangzhou 310027, China (e-mail: yinxunhu@zju.edu.cn; baominglei@zju.edu.cn; yiding@zju.edu.cn; yechengjing@zju.edu.cn).

P. Wang and L. Goel are with the Electrical and Electronic Engineering School, Nanyang Technological University, Singapore 639798 (e-mail: epwang@ntu.edu.sg; elkgoel@ntu.edu.sg).

DOI: 10.35833/MPCE.2022.000852

I. Introduction

WITH the growing need for improving energy utilization efficiency and reducing environmental pollution, integrated energy systems (IESs) have gained rapid development during the past few decades [1], [2]. One of the most important forms of IESs is the integrated electricity-heat system (IEHS) consisting of the electric power system (EPS) and the district heating system (DHS), which is responsible for providing customers with reliable energy supply to satisfy their service requirements [3]. For example, based on the energy flows in IEHSs, the heating service requirements of customers can be satisfied by electrical heating facilities or direct thermal power from DHS [4].

With the increasing interdependence between EPS and DHS, the customers may suffer energy-related service risks due to the random failures in IEHSs. For example, the malfunction of coupled components such as combined heat and power (CHP) units may result in the degradation or interruption of both the electric and the heat power supply for customers, which further affects the corresponding energy services of customers [5]. Besides, the sudden faults suffered by one energy subsystem will affect the services provided by the subsystem of the other energy form considering energy interactions, e.g., the blackout in EPSs can bring about the shortage of district heating services [6]. Since the energy service performances directly determine the energy usage satisfactions of customers, the above energy service risks in IEHSs could affect the utilities of customers. It is of significance to comprehensively analyze the reliabilities of IEHSs from the viewpoint of energy services for customers. Therefore, service-based reliability is defined in this paper as the ability of the energy system to provide adequate energy services for customers with a reasonable assurance of continuity and quality. It is extended from the traditional reliability definition of EPSs and applied to reliability measurement of IEHSs with different energy service forms.

The reliabilities of the individual energy subsystems, e.g., EPSs and DHSs, have been well studied in the previous research works [7], [8]. Recently, there have been several research works concerning the reliabilities of IESs considering the coupling relationship of the constituent energy subsystems. Reference [9] builds a capacity reliability model of IESs using a multi-dimensional matrix method. Reference

[10] develops a systematic framework to assess the reliability of energy supply in IESs considering the inter-relationships among multiple uncertainties. Reference [11] proposes a reliability analysis method for multi-agent IESs with fully distributed communication, which aims to protect data privacy between different stakeholders. Some research works focus on the reliabilities of the specific forms of IESs. For example, reliabilities of the integrated electricity-gas systems composed of EPSs and natural gas systems are analyzed in [12], [13]. In addition, there are also a few studies [5], [14], [15] concerning the reliabilities of IEHSs. Specifically, the reliability and availability models for IEHSs are developed in [5] based on the state spaces of different subsystems. Reference [14] evaluates the reliabilities of IEHSs considering the maximum output of heat pumps as the critical coupling devices. The reliabilities of different forms of energy supply including electricity and heat are analyzed in [15] by combining the state-space method and the probabilistic analysis of the Markov model. However, the previous studies mainly measure the reliabilities of IEHSs according to energy supply conditions such as the overall generating capacities or instant energy load curtailments in contingency states. These research works cannot characterize the energy service conditions directly perceived by customers. For example, the insufficient heat power supply can quickly lead to dissatisfaction of some industrial customers with strict temperature requirements, while the residential customers with relatively low requirements could still be satisfied for a while [16]. By comparison, the service-based reliability could consider the dynamic characteristics of energy services and is more related to the requirements and satisfactions of customers.

As the two forms of energy service for customers, the electric and heating services can show different dynamic characteristics in contingency states. In specific, the electric services would degrade instantaneously when the failure occurs, while the heating services would degrade gradually and the heating requirements of customers can be maintained for a period of time [17]. The dynamic degradation processes of heating services are mainly related to the thermal inertia at both the transmission side and the demand side [18], [19]. At the transmission side of IEHSs, the transfer delays in pipelines can slow down the failure propagation from heating sources to customers [20]. At the demand side of IEHSs, the thermal storage capabilities of buildings are also equivalent to buffers for the heat power supply shortage, which can lead to transient heat losses and maintain the satisfaction of thermal customers for a while [21]. Consequently, the thermal dynamics of both transmission and demand sides can significantly affect the energy services in contingency states of IEHSs, which need to be considered in the service-based reliability analysis.

There have been some previous research works [22]-[28] conducting the reliability researches considering thermal dynamics. Reference [22] conducts the reliability simulation of thermal dynamic processes inside the power plant. Reference [23] concentrates the reliability of heat power supply from hybrid energy sources while considering effects of thermal inertia. Nonetheless, the component-level methods in [22], [23] are not suitable for analyzing thermal dynamics in energy systems and their reliabilities. Reference [24] evaluates the reliability of district heating networks considering the dynamic influence of changeable external conditions. However, the studied object is just an individual heating system rather than an IEHS, where the electric and heat flows are strongly coupled and present different dynamic characteristics especially in contingency states. Recently, [25]-[28] have focused on the reliabilities of IEHS while characterizing thermal dynamics at different locations of heating systems. Reference [25] formulates the heat losses along the pipelines in heating networks but ignores the time-delay for heat power transmission and the dynamic phenomena at the demand side. In [26], [27], the thermal inertia of buildings is considered in reliability assessments of IEHS, but the transmission-side thermal dynamics in heating networks are not modelled. Although a relatively complete thermal dynamic model is given in [28], it is limited and inapplicable in practical situations without formulating variable hydraulic conditions in heating networks. In addition, all of the above research works do not consider the energy services for customers, which are unsuitable for the service-based reliability analysis.

In order to quantify the service-based reliabilities of IEHSs, the pertinent reliability indices are needed. The existing reliability indices for EPSs are usually steady-state which are utilized to reflect the system reliability levels over a long period [29]. In [30], the reliability indices for other energy-form systems, e.g., natural gas systems, are proposed by modifying traditional EPS reliability indices. Nonetheless, these steady-state indices mainly focus on the expected energy supply losses and the corresponding probabilities, which cannot accurately characterize the reliabilities related to the chronologically dynamic energy services. Besides, since the service-based reliabilities concentrate on the service satisfaction of customers derived from system operation, the energy service requirements of customers should be considered in the definition of the corresponding indices.

In order to bridge the research gaps, this paper contributes in the following aspects:

1) The service-based reliability of IEHS is firstly defined and analyzed in this paper. The system reliability is evaluated based on the energy service conditions of customers rather than the energy supply conditions in the traditional reliability research works.

2) The energy service performance of IEHS for customers in contingency states is modelled considering thermal dynamics. In specific, the nodal energy supplies are obtained from the optimal power and heat flow (OPHF) model under both variable hydraulic and thermal conditions, in which the transmission-side thermal dynamics are formulated. Then, the energy service performances for customers are further determined with the formulation of demand-side thermal dynamics.

3) A service-based reliability analysis framework for the IEHSs is proposed based on the time-sequential Monte Carlo simulation (TSMCS) technique. During the inner loop of the TSMCS, a hydraulic-thermal decomposition algorithm is embedded to realize the tractable calculation of OPHF model,

which characterizes the chronological impacts of thermal dynamics on service-based reliabilities.

4) Conventional steady-state reliability indices are re-defined to quantify the time-varying service-based reliabilities of IEHSs. The dynamic service performances and service satisfactions of customers are both considered in the definition of the indices to ensure the accuracy and effectiveness of reliability evaluation.

II. General Description for Impacts of Thermal Dynamics on Service-based Reliabilities of IEHSs

In this section, the impacts of thermal dynamics on service-based reliabilities of IEHSs are firstly described with the schematic diagram shown in Fig. 1. In IEHSs, EPSs and DHSs are interconnected through coupled components including CHP units and electric heating devices, and thermal dynamics exist in both transmission and demand sides, as shown in Fig. 1(a). The electric and heating energies supplied by IEHSs eventually come down to energy-related services for customers such as lighting services and space heating services [31]. The continuity and quality levels of performing these energy services are referred to as service performances, which can be measured by specific physical parameters. Here, the load power and temperature are used as measures of performances for the electric and heating services, respectively.

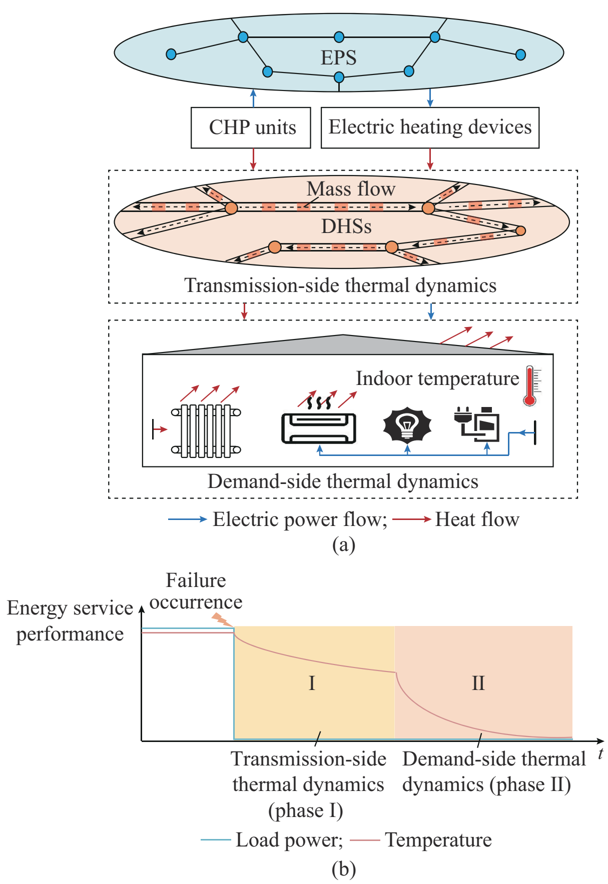

Fig. 1. Thermal dynamics in IEHSs and their impacts on service-based reliabilities. (a) Transmission-side and demand-side thermal dynamics in IEHSs. (b) Energy service performances affected by thermal dynamics.

In a certain contingency state, the energy service performances would be affected by thermal dynamics in IEHSs, as shown in the shaded area of Fig. 1(b). Failures in IEHSs generally lead to insufficient electric and heating supplies, which could cause the performance degradation of different energy services. After the occurrence of failures, the performance degradation of the electric services, e. g., lighting, is instant since the customers will perceive the load power interruption immediately. In contrast, the degradation of heating service performances is transient consisting of two phases, which are affected by thermal dynamics at transmission and demand sides, respectively. In specific, phase I denotes the period for failure propagation at the transmission side, during which the temperatures of customers vary slightly due to the thermal storage of pipelines. Besides, phase II denotes the period after the failure reaches the demand side, which reflects the dynamic heat loss due to the thermal inertia of buildings.

As analyzed above, the performances of energy services present dynamic variation processes in contingency states. With various kinds and degrees of failures, the dynamic performances would take different forms such as the slight degradation for minor disturbances and severe degradation for large failures in IEHSs. Considering the possible scenarios with different performances, the overall service-based reliability could be determined, which denotes the ability of IEHSs to provide adequate energy services for customers. Moreover, the reliability levels of IEHSs in this manner would be affected by thermal dynamics, which should be consequently considered in the service-based reliability analysis.

III. Modelling Energy Service Performances in Contingency States Considering Thermal Dynamics

To analyze the service-based reliabilities of IEHSs, the energy service performances in contingency states are modelled and calculated considering thermal dynamics in this section. Firstly, the reliability models of components in IEHSs are proposed to characterize the state transition processes, where both the electric and heat performances in each state are considered for coupled components especially. Then, the transmission-side and the demand-side thermal dynamics are considered, respectively, in the two stages for modelling the energy service performances in contingency states. Specifically, the contingency electric and heat power supply for customers at each node in IEHSs is determined considering the thermal storage of pipelines. According to the nodal contingency energy supply, the energy service performances of customers are measured considering thermal inertia of buildings.

A. Multi-state Reliability Models of Coupled Components

Random failures of coupled components (e. g., generator units, electric lines, pipelines) could make the IEHS enter the contingency state. To analyze the contingency performance of the IEHS, the reliability modelling of coupled components is conducted firstly. In practice, the components usually present more than two exclusive states (e. g., $M+1$

states) from perfectly functioning s_0 to complete failure s_M. The intermediate states of components $(s_1, s_2, \ldots, s_{M-1})$ are characterized by the partially functioning performances considering performance degradation [32]. Therefore, the multi-state reliability model can be formulated and each state corresponds to a certain performance level. The state space of a certain component can be described by the state transition matrix $\boldsymbol{S}$ [8]:

$$\boldsymbol{S}=\begin{bmatrix} 0 & \lambda_{0,1} & \cdots & \lambda_{0,M} \\ \mu_{1,0} & 0 & \cdots & \lambda_{1,M} \\ \vdots & \vdots & & \vdots \\ \mu_{M,0} & \mu_{M,1} & \cdots & 0 \end{bmatrix} \tag{1}$$

where $\lambda_{i,j}$ and $\mu_{i,j}$ are the failure rate and repair rate from states i to j, respectively.

Different from the other components related to one type of energy, the coupling components in IEHSs, e. g., CHP units and electric boilers (EBs), have both the electric and the heat performances. To comprehensively measure the performances of the coupling component in a certain state, a two-dimensional parameter represented as C_{EG}^s and C_{HG}^s can be used, where C_{EG}^s and C_{HG}^s denote the electricity and heat generation capacities in state s, respectively. Especially for electric heating devices such as EBs, C_{EG}^s is negative to describe the electric power consumption behavior. Therefore, the two-performance multi-state reliability model for coupling components can be developed, as shown in Fig. 2. In addition, there is a coupling relationship between C_{EG}^s and C_{HG}^s considering the working characteristics of coupling components, which will be modelled in the next subsection.

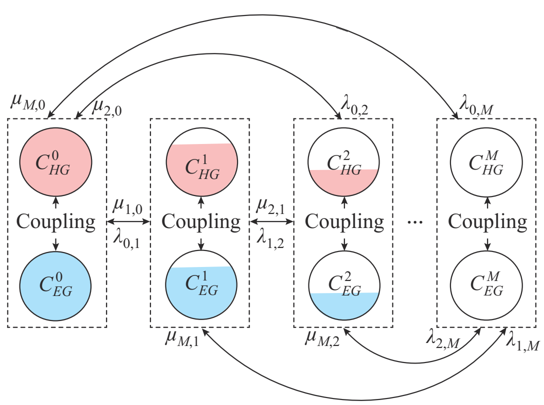

Fig. 2. Two-performance multi-state reliability model for coupling components.

B. Contingency Energy Supply Determination for Customers Considering Transmission-side Thermal Dynamics

In the contingency state, the IEHS will be re-dispatched and suffer the risk of energy load curtailment. Under this circumstance, the contingency energy supply for customers can be determined by calculating the energy load curtailment based on the thermal dynamic model of pipelines and the OPHF technique [3].

1) Thermal Dynamic Model of Pipelines

As modelled in the previous subsection, failures of coupled components may lead to the reduction of their heat generation capacities. After that, heating services could be maintained for a while considering the propagation time from the failure location to geographically distributed customers, which has been theoretically analyzed in Section II. Such dynamic process is related to the storage capability of insulated pipelines in IEHSs, which could be modelled based on the node method [19].

The basic idea of this method is to represent the outlet temperatures of pipelines using historic inlet temperatures [19]. The mass flow inside the pipeline is discretized into multiple blocks to characterize the transfer delays. The detailed modelling process is presented as follows.

Firstly, the outlet temperature is represented as the mean temperature of the outflowing mass flow blocks at the tail of the pipeline:

$$T_{p,out}^t=\alpha_1 T_{p,out1}^t+\alpha_2 T_{p,out2}^t \tag{2}$$

$$\begin{cases}\alpha_1=(M_1-\rho_p AL)/m_p\Delta t \\ \alpha_2=(M_2-M_1)/m_p\Delta t\end{cases} \tag{3}$$

where $T_{p,out1}^t$ and $T_{p,out2}^t$ are the temperatures of the two outflowing mass flow blocks in pipeline p; m_p is the mass flow rate in pipeline p; α_1 and α_2 are the proportion coefficients corresponding to the two outflowing mass flow blocks; M_1 and M_2 are the two masses for determining α_1 and α_2, respectively; and ρ_p, A, and L are the pipeline parameters denoting the mass density, cross-section area, and total length, respectively.

Then, the temperatures of outflowing mass blocks can be calculated by historic inlet temperatures at different time steps considering time delays in pipelines:

$$\begin{cases}T_{p,out1}^{t*}=T_{p,in1}^{t-o_1*} \\ T_{p,out2}^{t*}=T_{p,in2}^{t-o_2*}\end{cases} \tag{4}$$

$$\begin{cases}o_1=round[\rho_p AL/(m_p\Delta t)]-1 \\ o_2=o_1+1\end{cases} \tag{5}$$

where $T_{p,out1}^{t*}$, $T_{p,out2}^{t*}$ and $T_{p,in2}^{t-o_1*}$, $T_{p,in2}^{t-o_2*}$ are the current outlet temperatures and historic inlet temperatures of the two outflowing mass flow blocks without heat losses, respectively; and o_1 and o_2 are the integers for time intervals calculated by rounding the precise transfer delays.

Besides time delays, heat losses during heat transmission along the pipeline should also be characterized. Hence, inlet temperatures considering heat losses can be modelled as:

$$\begin{aligned}T_{p,in}^{t-o_1}&=\gamma_1(T_{p,in}^{t-o_1*}-T_{env})+T_{env} \\ T_{p,in}^{t-o_2}&=\gamma_2(T_{p,in}^{t-o_2*}-T_{env})+T_{env}\end{aligned} \tag{6}$$

$$\begin{cases}\gamma_1=\mathrm{e}^{-\lambda L_1/(m_p c_w)} \\ \gamma_2=\mathrm{e}^{-\lambda L_2/(m_p c_w)}\end{cases} \tag{7}$$

where $T_{p,in}^{t-o_1}$ and $T_{p,in}^{t-o_2}$ are inlet temperatures of pipeline p at times $t-o_1$ and $t-o_2$, respectively; γ_1 and γ_2 are the heat loss factors; T_{env} is the environment temperature of the pipeline; λ is the heat transfer coefficient; L_1 and L_2 are the equivalent lengths; c_w is the specific heat capacity of water; and * is a symbol for variables without considering heat losses.

Combining (2), (4), and (6), the relationship between the outlet and inlet temperatures considering both time delays and heat losses is formulated as:

$$T_{p,out}^{t}=\alpha_1\alpha_2 T_{p,in}^{t-o_1}+\gamma_1\gamma_2 T_{p,in}^{t-o_2}+(\alpha_1+\alpha_2-\alpha_1\gamma_1-\alpha_2\gamma_2)T_{env} \tag{8}$$

When the mass flow rate is fixed, α_1, α_2, γ_1, and γ_2 will become constant parameters and the relationship formulated in (8) will be linear. This feature will be used by the decomposition algorithm to solve the following optimal load curtailment model which integrates the formulated thermal dynamic model of pipelines. The detailed algorithm will be given in Section IV-B.

2) Optimal Load Curtailment Model of IEHSs Considering Transmission-side Thermal Dynamics

Based on the OPHF technique, the optimal load curtailment model of IEHSs is formulated which can determine the nodal contingency energy supply. The objective of the model is to minimize the total system operation cost in the contingency state s during the studied period:

$$\min f^{s}=\sum_{t}\left[\sum_{m}(O_{PG}(P_{mc}^{t,s})+O_{PG}(P_{mg}^{t,s})+O_{PL}(PC_{m}^{t,s}))+\sum_{i}(O_{HG}(H_{ic}^{t,s})+O_{HL}(HC_{i}^{t,s}))\right] \tag{9}$$

$\sum_{m}(O_{PG}(P_{mc}^{t,s})+O_{PG}(P_{mg}^{t,s})+O_{PL}(PC_{m}^{t,s}))$ denotes the cost related to nodal electric power supply, including the generation cost of CHP units and non-CHP thermal units along with the electric load curtailment cost. $\sum_{i}(O_{HG}(H_{ic}^{t,s})+O_{HL}(HC_{i}^{t,s}))$ denotes the cost related to nodal heat power supply considering both heat generation of CHP units and heat load curtailments. Moreover, the electric loads are divided into heating and non-heating loads considering the electric heating devices at the demand side, and the curtailment of the former can affect the heating service performances.

The objective function is subject to the constraints of the IEHS, including the coupled component constraints, DHS constraints, and EPS constraints. It should be noted that the superscripts s for variables in (9) are omitted for simplicity.

1) Coupled component constraints

Coupled components in IEHSs mainly include the CHP units and the electric heating devices such as EBs. Each coupled component generates the electric or heat power within C_{EG}^{s} or C_{HG}^{s} for a certain state as defined in Section III-A:

$$0\le P_{mc}^{t}\le C_{EG,c}^{s}\quad 0\le H_{ic}^{t}\le C_{HG,c}^{s} \tag{10}$$

$$0\le P_{ik}^{t}\le \left|C_{EG,ie}^{s}\right|\quad 0\le H_{ik}^{t}\le C_{HG,ie}^{s} \tag{11}$$

where P_{mc}^{t} and H_{ic}^{t} are the generated electric power and heat power of the CHP unit c, respectively; P_{ik}^{t} and H_{ik}^{t} are the consumed electric power and generated heat power of the EB k at time t, respectively; and $|\cdot|$ is the operator for calculating the absolute value.

Besides, the electric and heat energy behaviors for each state of these components are strongly coupled. Regarding the electric heating devices, the generated heat power is proportional to the consumed electric power, as denoted in (12). Regarding the CHP units, the coupling relation between electric and heat generation can be described by the polyhedron feasible operating region [33], which is formulated by the convex combination of extreme points in polyhedrons, as expressed in (13).

$$H_{ik}^{t}=\eta_k P_{ik}^{t} \tag{12}$$

$$\begin{cases} P_{mc}^{t}=\sum_{r=1}^{NR_c}\kappa_{c,r}^{t}P_{c,r} \\ H_{ic}^{t}=\sum_{r=1}^{NR_c}\kappa_{c,r}^{t}H_{c,r} \\ \sum_{r=1}^{NR_c}\kappa_{c,r}^{t}=1\quad 0\le\kappa_{c,r}^{t}\le 1, r\in\{1,2,...,NR_c\} \end{cases} \tag{13}$$

where η_k is the conversion efficiency of EB k; NR_c is the number of extreme points in polyhedron operating region of CHP unit c; $P_{c,r}$ and $H_{c,r}$ are the electric power and heat power corresponding to the r^{th} extreme point; and $\kappa_{c,r}^{t}$ is the variable for illustrating the operation point of CHP unit c.

Moreover, the generated heat power of the components can heat the mass flow at the nodes where they locate in IEHSs:

$$H_{ic}^{t}+H_{ik}^{t}=c_w m_i^{t}(T_{is}^{t}-T_{ir}^{t}) \tag{14}$$

where m_i^t is the mass flow rate at node i and time t; T_{is}^{t} and T_{ir}^{t} are the supply and return mass flow temperatures at node i, respectively.

2) DHS constraints

Similar to (14), in the heat load nodes, the heat load power of customers is satisfied by the heated mass flow of the connected pipelines in IEHSs:

$$HD_i^t-HC_i^t=c_w m_i^t(T_{is}^t-T_{ir}^t) \tag{15}$$

where HD_i^t and HC_i^t are the original heat load and the heat load curtailment at node i and time t, respectively.

In order to guarantee the heating service quality and prevent steam forming, temperatures of both supply water and return water are bounded as:

$$\begin{cases} T_{is}^{\min}\le T_{is}^{t}\le T_{is}^{\max} \\ T_{ir}^{\min}\le T_{ir}^{t}\le T_{ir}^{\max} \end{cases} \tag{16}$$

where $T_{is}^{\max}$, $T_{is}^{\min}$ and $T_{ir}^{\max}$, $T_{ir}^{\min}$ are the upper and lower boundaries of T_{is}^{t} and T_{ir}^{t}, respectively.

The temperature of the confluence node is the weighted average value of outlet temperatures in all pipelines ending at that node [33]:

$$\sum_{p\in S_i^{p,in}}T_{p,out}^{t}m_p^{t}=T_i^{t}\sum_{p\in S_i^{p,in}}m_p^{t} \tag{17}$$

where $S_i^{p,in}$ is the set of pipelines ending at node i; $T_{p,out}^{t}$ is the outlet temperature of pipeline p at time t; and T_i^t is the mixed temperature at node i and time t.

According to the Darcy-Weisbach equation [34], the pressure loss along pipelines is proportional to the square of mass flow rate, and the the pressure loss in a closed loop is euqual to zero:

$$\begin{cases} \Delta\pi_p^{t}=\zeta_p(m_p^{t})^2 \\ \sum_{p\in S_{p,loop}}K_p\Delta\pi_p^{t}=0 \end{cases} \tag{18}$$

where $\Delta\pi_p^t$ is the pressure loss along pipeline p at time t; ζ_p is the coefficient of pressure loss in pipeline p; $S_{p,loop}$ is the set of pipelines forming a closed loop; and $K_p=1$ denotes that the directions of mass flow in pipeline p and the loop are consistent, while $K_p=-1$ denotes that the two directions are opposite.

3) EPS constraints

The EPS operation in the contingency state mainly subjects to the following constraints.

$$P_{mg}^{\min}\leq P_{mg}^t\leq P_{mg}^{\max} \tag{19}$$

$$-RD_{mg}\leq P_{mg}^t-P_{mg}^{t-1}\leq RU_{mg} \tag{20}$$

$$\sum_g P_{mg}^t+\sum_c P_{mc}^t=\sum_m[(PD_{m0}^t-PC_{m0}^t)+(PD_{mH}^t-PC_{mH}^t)] \tag{21}$$

$$P_l^t=\sum_g \pi_{l\text{-}g}P_{mg}^t+\sum_c \pi_{l\text{-}c}P_{mc}^t-\sum_m \pi_{l\text{-}m}[(PD_{m0}^t-PC_{m0}^t)+(PD_{mH}^t-PC_{mH}^t)] \tag{22}$$

$$-P_l^{\max,t}\leq P_l^t\leq P_l^{\max,t} \tag{23}$$

where $P_{mg}^{\max}$ and $P_{mg}^{\min}$ are the upper and lower boundaries for power output of non-CHP generation unit g at node m, respectively; RU_{mg} and RD_{mg} are the upward and downward ramping capabilities of non-CHP generation unit g at node m, respectively; PD_{m0}^t, PD_{mH}^t and PC_{m0}^t, PC_{mH}^t are the original non-heating and heating electric loads and the corresponding load curtailments at node m, respectively; $\pi_{l\text{-}g}$, $\pi_{l\text{-}c}$, and $\pi_{l\text{-}m}$ are the shift distribution factors from unit g, unit c, and node m to line l, respectively; and $P_l^{\max,t}$ is the transmission capacity determined by dynamic thermal rating (DTR) [35]-[38]. Equation (19) is the power output constraint for generation units. Equation (20) denotes the ramping constraint for generation units. Equation (21) represents the power balance in EPS. Equation (22) formulates the power flow P_l^t of line l. Equation (23) denotes the line capacity constraint.

Since the conventional static thermal rating (STR) generally sets the fixed low ratings of power lines with the conservative assumption of weather conditions, it could lead to the underutilization of line capacities [37]. To tackle this problem, DTR is used to obtain the dynamic line capacity values based on the real-time weather data. In this manner, more potential line rating flexibility can be offered, which will benefit the electric power supply in EPS in contingency states. According to IEEE 738 standard [39], the DTR model can be represented as a heat balance equation for the line:

$$H_c(T_{line},T_{env},V_{wind},\varphi)+H_r(T_{line},T_{env})=H_s+I^2R(T_{line}) \tag{24}$$

where T_{line}, T_{env}, V_{wind}, and φ are the line conductor temperature, environment temperature, wind speed, and incident wind angle, respectively; I is the line current; R is the line conductor resistance changing with T_{line}; H_c is the convection heat loss as a function of T_{line}, T_{env}, V_{wind}, and φ; H_r is the radiated heat loss as a function of T_{line} and T_{env}; and H_s and $I^2R(T_{line})$ are the heat gains from solar radiation and line conductivity, respectively. In DTR model, the line rating denotes the current $I^{\max}$ that yields the maximum allowable conductor temperature $T_{line}^{\max}$ with the given weather parameters, which further determines the line capacity $P_l^{\max}$ in (23).

After obtaining the nodal load curtailment in the formulated optimization problem (9)-(23), the contingency energy supply for customers can be calculated using (25) and (26). Here, the contingency electric power supply is divided into the heating and non-heating parts, as represented in (26).

$$\begin{cases}PD_{m0,con}^t=PD_{m0}^t-PC_{m0}^t\\PD_{mH,con}^t=PD_{mH}^t-PC_{mH}^t\end{cases} \tag{25}$$

$$HD_{i,con}^t=HD_i^t-HC_i^t \tag{26}$$

where $PD_{mH,con}^t$ and $PD_{m0,con}^t$ are the heating and non-heating parts of the contingency electric power supply at node m, respectively; and $HD_{i,con}^t$ is the contingency heat power supply at node i.

C. Energy Service Performance Determination for Customers Considering Demand-side Thermal Dynamics

According to the contingency energy supply conditions in the previous stage, the energy service performances of IEHSs for customers can be further calculated. Since the electric service interruptions are mostly static, the corresponding contingency performances can be measured by the supplied load power directly. In contrast, the heating service performances are greatly affected by the demand-side thermal dynamics, which are measured by physical variables related to time-varying temperatures in this paper.

In the demand side of IEHSs, the heating services are mainly provided by the heat power from DHSs. Besides, for customers equipped with electric heating devices, the partial heat power demands can also be satisfied by the electric power supply. Therefore, the total contingency heat power supply for customers is expressed as:

$$\begin{cases}HD_{iALL,con}^t=HD_{i,con}^t+HD_{im,con}^t\\HD_{m,con}^t=\eta_m\cdot PD_{mH,con}^t\end{cases} \tag{27}$$

where $HD_{iALL,con}^t$ is the total contingency heat power supply for customers at heat node i; $HD_{im,con}^t$ is the heat power at node i converted from the electric power at node m; and η_m is the conversion efficiency.

When the heat power supply is insufficient, the heat loss of the building is a slow and transient process due to the insulation structures, which can be demonstrated by the dynamic indoor temperatures. Since the heating service satisfaction of customers is usually determined by the indoor temperatures, they are utilized as one of the physical variables to measure the heating service performances in contingency states of IEHSs, as shown in Fig. 3.

The indoor temperature variation is related to both the contingency heat power supply from the IEHSs and the heat exchange with the outdoor environment, which is formulated utilizing the first-order equivalent thermal parameter (ETP) model [40]:

$$HD_{iALL,con}^t=C_{ib}\frac{\mathrm{d}T_{ib}}{\mathrm{d}t}+\frac{T_{ib}-T_{env}}{R_{ib}} \tag{28}$$

where T_{ib} is the indoor temperature of the equivalent building b at node i; and C_{ib} and R_{ib} are the heat capacity and thermal resistance [41] of the equivalent building b, respectively.

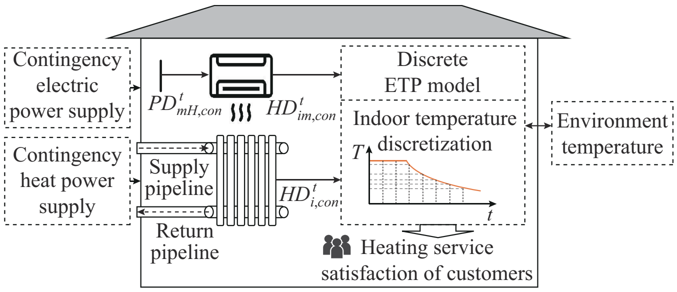

Fig. 3. Thermal dynamic model of buildings in the demand side.

Furthermore, the variation of the indoor temperature ΔT^t_{ib} at each time slot is obtained by discretizing the differential equations as modelled in (28).

Obviously, the indoor temperature variation is limited by the time interval as illustrated in (29), and the temperature would reduce over time before the heat equilibrium is achieved. In other words, the heating services will not be lost immediately from the perspective of customers.

$$\Delta T^t_{ib} = T^{t+1}_{ib} - T^t_{ib} = \frac{HD^t_{iALL,con} R_{ib} - (T^t_{ib} - T_{env})}{C_{ib} R_{ib}} \Delta t \tag{29}$$

To reflect dynamic energy losses during the temperature degradation period, the heating service performances also need to be measured by power. Hence, the equivalent heat load power EHD^t_i modelled by temperatures is used as another physical variable for heating service performances, which is defined as follows:

$$EHD^t_i = \frac{T^t_{ib} - T^t_{env}}{R_{ib}} \tag{30}$$

D. Analysis of Factors Affecting Dynamic Processes

In the above subsections, thermal dynamics have been characterized in the two stages for determining energy service performances in contingency states. These dynamic processes are equivalent to buffers for the energy supply shortage in the contingency states, which are beneficial for the IEHS to provide reliable energy services. Therefore, it is valuable to analyze the factors that affect the dynamic processes for investigating the potential improvement of the service-based reliabilities.

According to the specific thermal dynamic models, there are several factors that could affect the transmission-side and demand-side thermal dynamics. Regarding the transmission-side thermal dynamics as formulated in (2)-(8), the factors include the pipeline parameters such as the length L and the cross-section area A. These factors for dynamic processes are related to the failure propagation time in the transmission side of IEHS in contingency states. In addition, based on the model (28) and (29), the factors affecting the demand-side dynamic processes mainly include the heat capacity C and thermal resistance R of the equivalent buildings. These factors determine the thermal inertia of customers, which are related to the dynamic service losses when the energy supply is insufficient. In a word, all of the above factors would have impacts on the service-based reliability levels of IEHS through different dynamic processes in contingency states.

IV. Service-based Reliability Analysis Framework for IEHSs Using TSMCS Techniques

A. Service-based Reliability Indices

The conventional indices such as the loss of load probability and the expected energy not supplied have been widely used to evaluate the reliability of the EPSs [29]. In this paper, they are re-defined as dynamic indices and extended to IEHSs for service-based reliability analysis according to the energy service performances modelled in the previous section.

Firstly, the equivalent heat load power and dynamic temperatures are used to define the reliability indices for heating services, as shown in Fig. 4. As mentioned in Section III, the equivalent heat load power EHD^t_i can measure the heating service performances in contingency states. Hence, the equivalent heat load curtailment EHC^t_i can be further calculated by subtracting EHD^t_i from the original total heat load power HD^t_{iALL}:

$$EHC^t_i = HD^t_{iALL} - EHD^t_i \tag{31}$$

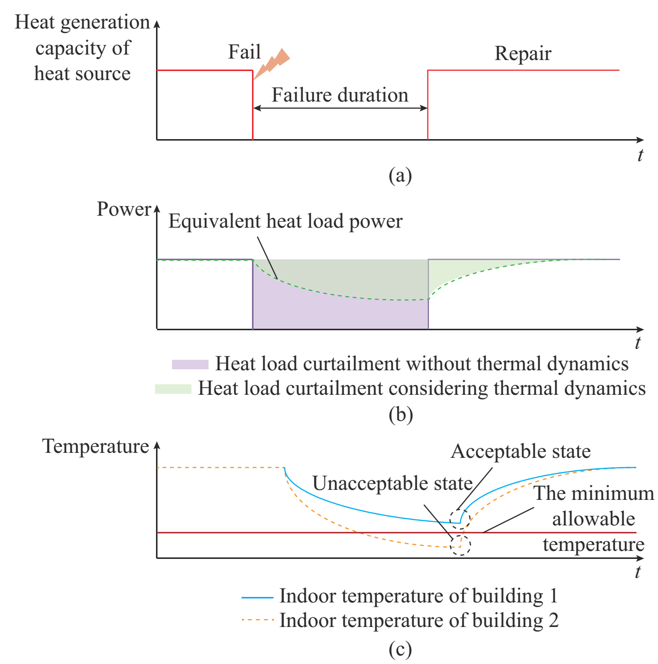

Fig. 4. Equivalent heat load power and dynamic temperatures used for defining service-based reliability indices. (a) Heat generation capacity of heat source. (b) Heat load curtailment considering thermal dynamics. (c) Dynamic temperatures of buildings.

Different from the conventional static load curtailment, the equivalent heat load curtailment can reflect the demand-side dynamic heat loss processes, as shown in Fig. 4(b). On this basis, the expected heating service not supplied $EHSNS^t$ is defined as:

$$EHSNS^t = \frac{\sum_{i=1}^{N_I} \sum_{n=1}^{N_A} \int_0^t EHC^\tau_{i,n} \mathrm{d}\tau}{N_A} \tag{32}$$

where $EHC^\tau_{i,n}$ is the equivalent heat load curtailment at node i and time τ at the n^{th} iteration of TSMCS; N_A is the sampling number of TSMCS; and N_I is the number of heat nodes in the IEHS.

Moreover, the failure probability regarding heating services with dynamic performances is not suitable to be calculated by simply judging the occurrence of load curtailment. Instead, dynamic temperatures are used to achieve the accurate judgement which is commonly related to service satisfaction of customers, as explained in Fig. 4(c). In general, customers would not perceive the failure of heating services if T_{ib}^{t} is higher than their acceptable boundary $T_{ib}^{\min}$. As shown in Fig. 4(c), since the temperature in building 1 is always higher than the acceptable boundary value due to the great thermal inertia, customers would not perceive the service failure during the whole period. In contrast, customers of building 2 would perceive the failure since the temperature is lower than the acceptable boundary value for a period, during which time their heating service requirements cannot be satisfied by IEHS. Based on the dynamic temperatures, the loss of heating service probability $LOHSP^{t}$ is defined by comparing $T_{ib,n}^{t}$ and $T_{ib}^{\min}$:

$$LOHSP^{t}=\frac{\sum_{n=1}^{N_A} If\left(\sum_{i=1}^{N_I} If\left(T_{ib}^{\min}-T_{ib,n}^{t}\right)\right)}{N_A} \tag{33}$$

where $If(x)$ is defined as a sign function, and $If(x)=1$ when $x>0$, and $If(x)=0$ when $x\leq 0$; and $T_{ib,n}^{t}$ is the indoor temperature of the equivalent building b at node i and time t at the n^{th} iteration of TSMCS.

Since the electric service performances are measured by the supplied load power in contingency states, the corresponding reliability indices are calculated according to the time-varying nodal load curtailment. Specifically, the loss of electric service probability $LOESP^{t}$ and the expected electric service not supplied $EESNS^{t}$ of the EPS can be expressed as:

$$LOESP^{t}=\frac{\sum_{n=1}^{N_A} If\left(\sum_{m=1}^{N_M} PC_{m0,n}^{t}\right)}{N_A} \tag{34}$$

$$EESNS^{t}=\frac{\sum_{m=1}^{N_M}\sum_{n=1}^{N_A}\int_{0}^{t} PC_{m0,n}^{\tau}\,\mathrm{d}\tau}{N_A} \tag{35}$$

where N_M is the number of nodes in the IEHS.

B. Algorithm to Solve Optimal Load Curtailment Model

Since the hydraulic conditions, e.g., mass flow rate, and thermal conditions, e.g., supply temperature, can all be variable, there are several non-linear terms in DHS constraints (14)-(17). Besides, the pipeline dynamic model formulated in (2)-(8) is also non-convex. As a result, it would bring about the computational burden when solving the optimal load curtailment model of IEHSs formulated in Section III-B. Note that both these DHS constraints and the pipeline dynamic model will be linear and convex when the mass flow rates are fixed. On this basis, a hydraulic-thermal decomposition algorithm [42] is used to decompose the model into two linear programming problems. The procedures of the algorithm are listed as follows, where ϑ is the temperature deviation threshold.

Algorithm 1: hydraulic-thermal decomposition algorithm

1: Set the index $it=0$, and set the temperature variables to their lower boundaries $\boldsymbol{T}^{it}=\boldsymbol{T}^{\min}$
2: **while** TRUE **do**
3: Determine the heat losses at the transmission side and obtain the optimal output of heat sources satisfying the summation of heat loads and losses
4: Determine the mass flow rate variables $\boldsymbol{m}^{it}$ using (14), (15) and (17), (18)
5: Taking the mass low rates as the fixed values $\boldsymbol{m}^{t}=\boldsymbol{m}^{it}$, solve the optimal load curtailment model (2)-(26)
6: Update the temperature variables $\boldsymbol{T}^{it}$
7: **if** $\left|\boldsymbol{T}^{it}-\boldsymbol{T}^{it-1}\right|\leq\vartheta$ **then**:
8: Stop **while** loop, and output the solutions for index it
9: **else**
10: Set $it=it+1$, $\boldsymbol{T}^{it}=(\boldsymbol{T}^{it}+\boldsymbol{T}^{it-1})/2$, and return to **2**
11: **end if**
12: **end while**

C. Reliability Evaluation Procedures

The TSMCS technique is used to evaluate service-based reliabilities through numerous iterative simulations for the IEHS. At each simulation, the system state sequence is created during the study period ST based on the state sampling of components, and then the energy service performances of IEHS are further measured. At the last simulation, the proposed indices could be obtained as the final service-based reliability evaluation results for IEHS.

According to the focused time scale, the reliability could be evaluated for either the long term or the short term. Compared with long-term reliability, the short-term reliability could accurately incorporate the time-varying system operating conditions, which is consistent with the concept of operational reliability [43]. In the reliability evaluation framework, the ST of TSMCS can be chosen according to the specific research requirements [44]. And using TSMCS technique for short-term reliability analysis, which is realized by setting ST to hours or days, has been applied in many existing studies such as [45]-[47]. In this paper, the researched service-based reliability is more related to the operational phase when the dynamic characteristics of energy services are significant. Hence, ST can also be set as short-term timeframe, e.g., one week, and the proposed time-varying service-based reliability indices can be obtained using (31)-(35). In spite of this, the long-term reliability could also be assessed by setting a long ST, e.g., one year, which is generally measured by the time-independent reliability indices [43].

Based on the strong law of large numbers and the central limit theorem, the TSMCS will converge after a certain number of iterative simulations and the solution could satisfy the confidence level [44]. When TSMCS is applied in reliability evaluation, the variance coefficient of reliability indices can be used to measure the confidence level, which is usually regarded as the stopping criterion of TSMCS [44]. When the number of simulations is large enough, the variance coefficient will be less than the set criterion value and the TSMCS process will stop.

The flowchart for evaluating service-based reliabilities is as follows.

Step 1: input initial parameters of components in IEHS. Build the multi-state reliability models as expressed in (1) of the components, where C_{EG}^{s} or C_{HG}^{s} is used to represent the component performance in each state.

Step 2: suppose all the components perform perfectly in the initial time and determine the initial operation condition of IEHS. Set the iteration index $n=1$.

Step 3: conduct the TSMCS sampling for components and create their state sequences during the whole simulation period. Determine the contingency state of IEHS according to the state sequences of components.

Step 4: obtain the nodal electric and heat power supply in the contingency state of IEHS by solving the optimal energy load curtailment model represented as (2)-(26) and utilizing the hydraulic-thermal decomposition algorithm in Section IV-B.

Step 5: measure the energy service performances for customers using (27)-(30) according to the contingency nodal power supply obtained in *Step 4*.

Step 6: achieve the service-based reliability indices defined as (31)-(35) according to the energy service performances measured in *Step 5*.

Step 7: calculate the variance coefficients and check the stopping criterion presented in (36). If (36) is satisfied for the whole period, go to *Step 8*; otherwise, set $n=n+1$ and go back to *Step 3* for the next iteration.

$$\theta^{t}=\max\left(\frac{\sqrt{V(EESNS^{t})}}{EESNS^{t}},\frac{\sqrt{V(EHSNS^{t})}}{EHSNS^{t}}\right)\le\theta^{set} \tag{36}$$

where θ^{t} is the variance coefficient at time t; θ^{set} is the corresponding criterion value for stopping TSMCS; and $V(EESNS^{t})$ and $V(EHSNS^{t})$ are the variances of $EESNS^{t}$ and $EHSNS^{t}$, respectively.

Step 8: output the service-based reliability indices of the IEHS obtained in the final iteration.

V. Case Studies

The proposed method is tested on an IEHS which contains a 30-bus EPS modified from [48] and a meshed 32-node DHS modified from [49]. The topology of the test IEHS is shown in Fig. 5. There are 4 non-CHP thermal units (termed as G1-G4), 41 branches, and 20 electric loads in the EPS, while 32 pipelines and 18 heat loads are included in the DHS. The proportion of the heat loads for space heating services is 80%. The electric loads and other heat loads are used for the energy services with negligible dynamic characteristics, e.g., lighting and cooking services. Moreover, the coupled components in the test system include 2 CHP units (termed as CHP1 and CHP2) and one EB. The CHP units are extraction-condensing units, located at electric nodes 2 and 8 and heat nodes 31 and 1, respectively. The EB is located at electric node 27 and heat node 32.

The reliability parameters of the components in the test system are presented in Tables I and II [5], [7], [15]. The CHP units are represented as the four-state Markov model with same parameters, and the transition rates between different states are shown in Table I. As the coupled components, the capacities (C_{EG}^{s}, C_{HG}^{s}) of CHP units at their four states s_0-s_3 are (10 MW, 8 MW), (8 MW, 6.5 MW), (4 MW, 3.5 MW), (0, 0), respectively. Besides, the non-CHP units and the EB are represented as binary Markov models, and their reliability parameters are provided in Table II.

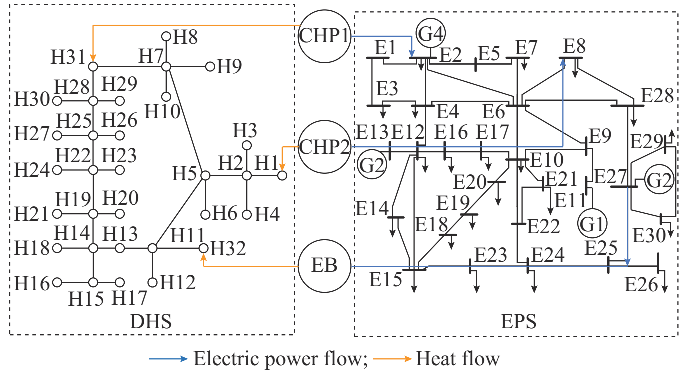

Fig. 5. Topology of test IEHS.

TABLE I
RELIABILITY PARAMETERS OF CHP UNITS

State	s_0	s_1	s_2	s_3
s_0		0.0022	0.0022	0.0011
s_1	0.020		0.0010	0.0021
s_2	0.020	0.0010		0.0021
s_3	0.020	0.0100	0.0100	

TABLE II
RELIABILITY PARAMETERS OF NON-CHP UNITS AND EB

Component	$\lambda_{0,1}$ (1/hour)	$\mu_{1,0}$ (1/hour)	C_{EG}^{s} (MW)	C_{HG}^{s} (MW)
G1	0.0021	0.050	10	10
G2	0.0011	0.020	16	16
G3	0.0010	0.025	16	16
G4	0.0022	0.020	20	20
EB	0.0021	0.050	8	8

The original electric and heat loads in the IEHS are set to their peak values. The equivalent heat capacities of buildings are 0.1 MWh/°C. The initial indoor temperature, environment temperature, and the minimum acceptable temperature of customers are 24 °C, –4 °C, and 14 °C, respectively. The modeling and simulations are conducted by MATLAB R2018a, which is performed on a computer with an 1.80 GHz Intel® Core™ i7-8550U and 8 GB memory. With the linearization techniques, the formulated model can be converted to the linear form and solved by IBM CPLEX solver. To demonstrate the effectiveness of the proposed method, five cases are carried out as follows.

A. Case 1: Energy Service Performances in Contingency State with Effect of Thermal Dynamics

This case study is performed in a specific contingency state to demonstrate the energy service performances of the test system utilizing the proposed method. The study period and the time interval are 72 hours and 15 min, respectively.

The contingency state of the test system is caused by the complete failure of CHP1 from $t=6.75$ hours to $t=33.75$ hours, when C_{EG}^{s} and C_{HG}^{s} are decreased to zero. The computation time of this case is 6.5 s, which is equivalent to the required time for a single simulation of TSMCS. The simulation results in this contingency state are presented as follows.

Firstly, the nodal electric and nodal equivalent heat load curtailments (PC and EHC) at some typical nodes are shown in Fig. 6, which illustrates the power-measured service performances of IEHS. As can be observed in Fig. 6, these two kinds of load curtailments present significant differences, characterizing the electric and heating service performances, respectively.

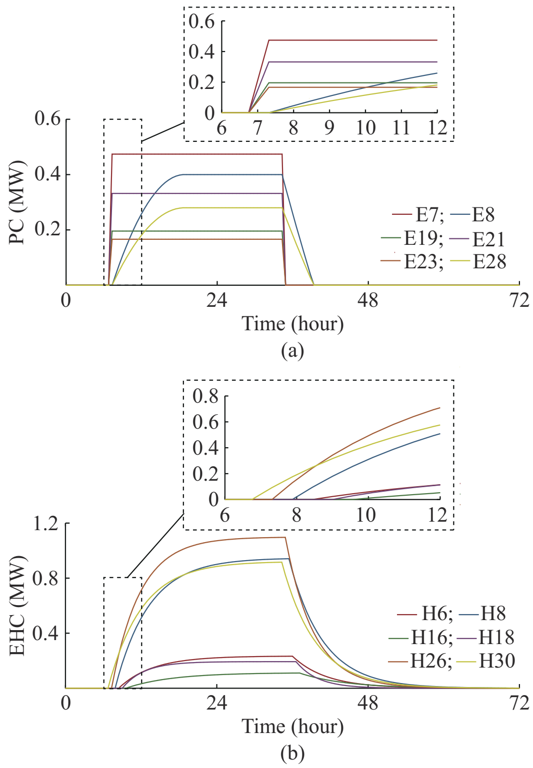

Fig. 6. Nodal electric and nodal equivalent heat load curtailments. (a) Nodal electric load curtailments. (b) Nodal equivalent heat load curtailments.

Regarding the heating service performances, the nodal equivalent heat load curtailments have transient forms with the contingency heat power supply. On the one hand, the dynamic variations can be observed for these nodes during the failure period, which originate from the thermal inertia of buildings. On the other hand, the delay times of load curtailments can be observed from the enlarged view for the initial failure period, which result from the transfer delays of pipelines. These time delays are related to the distances from the failure location to different heat nodes. For heat node 30 (H30) near CHP1, the delay time is only 34 min. However, it reaches 2.81 hours for heat node 16 (H16) with a long distance from CHP1.

Regarding the electric service performances, the load curtailments at different electric nodes present distinct patterns. On the one hand, most of the loads at electric nodes are curtailed immediately at the beginning of the failure period with the contingency electric power supply. On the other hand, different from the stable values of load curtailments at most electric nodes, load curtailments at some electric nodes such as E8 and E28 have transient processes and are delayed for about 34 min. These load curtailments are caused by the decrease of the electric power output of CHP2. When CHP1 fails, CHP2 is re-dispatched and increases its heat power output to compensate for the heat power supply shortage because of the higher priority of heat load. At the same time, the electric power output of CHP2 has to be decreased due to the electricity-heat coupling feature of the extraction-condensing CHP unit, and some electric nodal loads are consequently curtailed. Since the electric power output of CHP2 is related to the heat loads, these electric load curtailments are indirectly affected by thermal dynamics and thus present transient patterns.

As another measure for heating service performances, the indoor temperatures of buildings at the above-mentioned heat nodes are shown in Fig. 7. It is obvious that some thermal customers with contingency heat power supply can still accept this contingency state. For instance, the minimum indoor temperatures at the heat nodes H6, H16, and H18 are 18.2 ℃, 20.3 ℃ and 20.7 ℃ respectively, which are higher than the minimum allowable temperature. Accordingly, indoor temperatures at these nodes are always within the acceptable temperature zone, and this contingency state can be viewed as the acceptable state for thermal customers during the whole simulation period. On the other hand, the indoor temperatures of buildings at H8, H26, and H30 drop rapidly and are lower than the minimum allowable temperature from 10.13 hours to 39.38 hours. During this period, the thermal comfort of customers at these nodes is compromised and the state is unacceptable for them. It should be noted that although CHP1 is repaired at $t=33.75$ hours, the failure state for customers continues for about 5.63 hours because of the temperature recovery processes of buildings. Therefore, considering energy service satisfactions of customers, judgment methods of the customer acceptances for the electric and heating service performances in contingency states are quite different. The acceptances for electric service performances can be simply judged by the appearance of electric load curtailments, while the acceptances for heating service performances can be judged by the indoor temperatures more specifically.

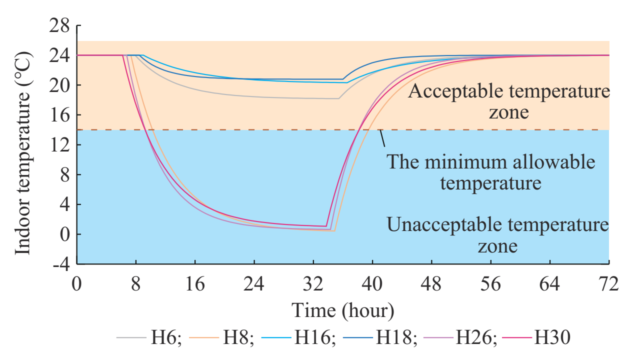

Fig. 7. Indoor temperatures of buildings.

B. Case 2: Service-based Reliability Evaluation Results

In the second case, the service-based reliability indices of the test system are calculated in two scenarios based on the proposed framework. Scenario A neglects the transmission- and demand-side thermal dynamics, which are modelled in Scenario B. The study period and the time interval are one week and 15 min, respectively. The tolerance level of variance coefficient is $\theta^{set}=0.05$.

The computation time of TSMCS is presented in Table III. Such time performance is acceptable in real application, which allows the system operator to conduct the service-based reliability analysis in the day ahead. In the last iterations of two scenarios, the maximum coefficients of variance θ^t are 0.0492 and 0.0497, both of which are lower than the tolerance level θ^{set}. Hence, the stopping criterion (36) is satisfied, which indicates the convergences of TSMCS in two scenarios.

TABLE III
COMPUTATION TIME OF TSMCS

Scenario	Number of iterations	Total time (hour)
A	4135	6.09
B	4322	8.16

The LOESP and LOHSP and EESNS and EHSNS in two scenarios are presented in Figs. 8 and 9, respectively. It can be observed that all the reliability indices in Scenario B are smaller than those of Scenario A, which means that the service-based reliabilities of IEHS are improved with the consideration of thermal dynamics. The improvement results from the energy storage capability behind thermal dynamic phenomena which slows down the degradation of energy service performances in the contingency states. Moreover, compared with the electric service based indices, the effects of thermal dynamics on heating service based reliability indices, i.e., LOHSP and EHSNS, are more prominent. During the initial period, the two indices remain at low levels close to zero in Scenario B, which corresponds to the delay time of service performances analyzed in Case 1.

Regarding the evaluation results for the whole study period, it can be observed from Fig. 8 that the LOESP and LOHSP curves in Scenario B exceeds the curves in Scenario A after t equals to 108 hours and 96 hours, respectively. This is because the repair of the faults in contingency states can be captured in the one-week simulation. During these repair periods, the unacceptable states for thermal customers would increase due to the temperature recovery processes as shown in Fig. 7. However, as shown in Fig. 9, the curves of EESNS and EHSNS in Scenario B are below the curves in Scenario A all the time, which is consistent with the results at the initial period. And the greatest differences of these two indices for the whole period between Scenario A and B are 1.58 and 3.59 MWh, respectively. This means that the expected energy service losses are reduced from the perspective of customers, thus thermal dynamics can lessen the cumulative service damage in IEHSs and improve the service-based reliabilities.

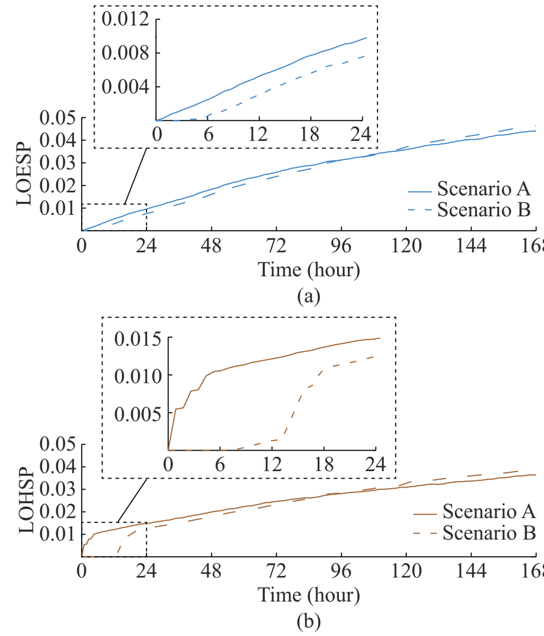

Fig. 8. LOESP and LOHSP in two scenarios. (a) LOESP. (b) LOHSP.

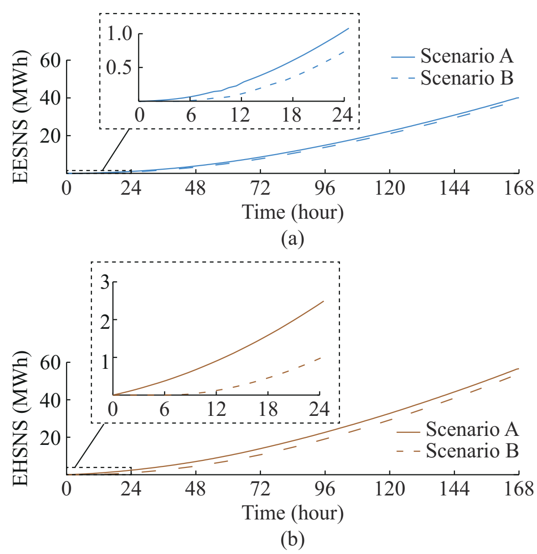

Fig. 9. EESNS and EHSNS in two scenarios. (a) EESNS. (b) EHSNS.

C. Case 3: Impacts of Thermal Dynamic Factors on Reliability of IEHS

As analyzed in Section III-D, thermal dynamics could be affected by several factors such as the pipeline parameters at the transmission side and the equivalent building parameters at the demand side. In this case, the impacts of the typical factors on the reliability of IEHS are investigated through different scenarios. Except for the studied factors, other settings in this case are the same as those in Scenario B of Case 2.

Firstly, three scenarios are considered and distinguished by different pipeline lengths in IEHS, which belong to the factors for the transmission-side thermal dynamics. In these scenarios, the pipeline lengths are set to be 0.5, 1.0, 2.0 times of original values, respectively. The LOESP and

LOHSP for different pipeline lengths are shown in Fig. 10. It is illustrated that both the LOESP and LOHSP indices will decrease if the pipelines are longer, indicating the probabilities reduction of unsatisfactory or unacceptable service from the viewpoint of customers. For example, when pipeline lengths change from 0.5 to 2.0 times, the LOESP at $t=18$ hours decreases by 45% from 0.0077 to 0.0042 while the LOHSP at the same time decreases by 78% from 0.0121 to 0.0027. Besides, in the third scenario, the two indices remain at low levels close to zero for the longest time during the initial period, reaching 10 and 13 hours, respectively.

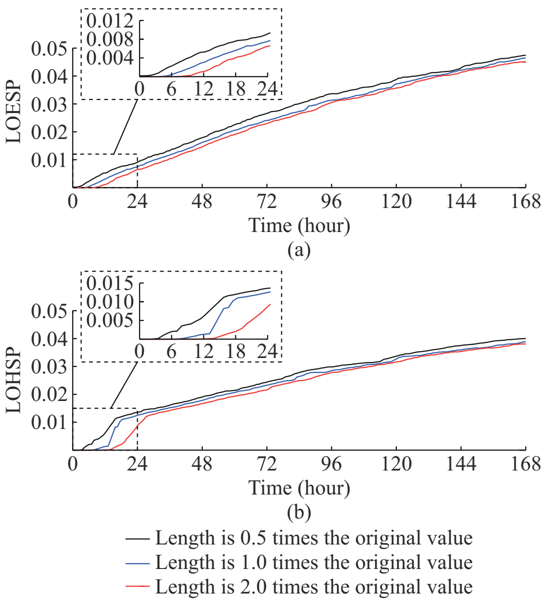

Fig. 10. LOESP and LOHSP for different pipeline lengths. (a) LOESP. (b) LOHSP.

In addition, the impacts of the heat capacity of the equivalent buildings, as the factor for the demand-side thermal dynamics, are also evaluated in this case. There are also three scenarios where the heat capacity levels of the equivalent buildings in IEHS are set to be 0.5, 1.0, and 2.0 times the original values respectively. The indices EESNS and EHSNS in these scenarios are used to illustrate the reliability results, as shown in Fig. 11. Similar to the scenarios for the pipeline length factor, the reliability indices tend to reduce with the increase of heat capacity levels. At the end of the study period when $t=168$ hours, the differences of EESNS and EHSNS for heat capacity levels of 0.5 and 2.0 times are 5.60 and 9.46 MWh, respectively. The reduction proportions of the two indices are 14% and 18%, respectively, indicating the decline of the cumulative service damages in IEHS.

In summary, the factors for both the transmission-side and demand-side thermal dynamics could affect the reliability of IEHS, since they determine the potential energy storage capabilities of the system. Either the longer pipelines or the larger building heat capacities correspond to the greater energy storage capabilities with more significant dynamic processes. Under these circumstances, the energy service provisions for customers are better ensured in contingency states and thus the reliability levels of IEHS could be improved.

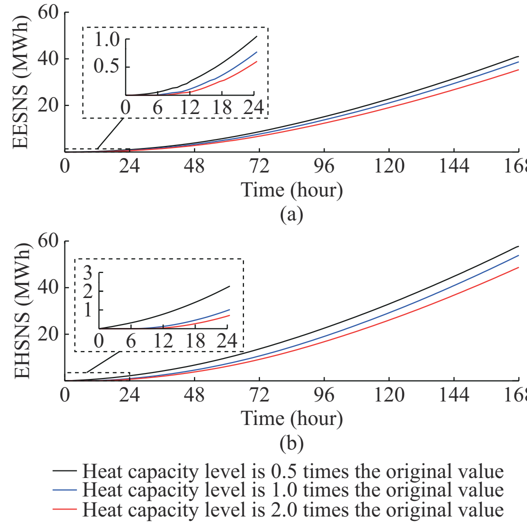

Fig. 11. EESNS and EHSNS for different heat capacity levels of equivalent buildings. (a) EESNS. (b) EHSNS.

D. Case 4: Impacts of DTR on Reliability of IEHS

Apart from thermal dynamic factors, the DTR could also have impacts on the reliability of IEHS, which is investigated in Case 4. Here, two scenarios are considered where the STR and DTR are applied in IEHS, respectively. The maximum allowable conductor temperature of power lines is set to be 100 ℃. The conductor coefficients and weather data for DTR are referred to [36] and [39]. Other simulation settings in this case are the same as those in Scenario B of Case 2.

The reliability indices EESNS and EHSNS and their differences in STR and DTR are shown in Fig. 12. The results indicate that both EESNS and EHSNS indices of the DTR scenario decrease significantly compared with those of the STR scenario, and the differences between two scenarios grow with time. The reason is that the capacities of power lines are raised by DTR, which could relieve the transmission congestions in the contingency states and benefit the energy service provisions in IEHS. In addition, the reliability indices and their differences in STR and DTR scenarios are also presented in Fig. 12. It can be observed that the difference of EESNS at each time is larger than that of EHSNS. At $t=168$ hours, the EESNS difference is 7.82 MWh, accounting for 20% of the EESNS value in STR scenario. At the same time, the EHSNS difference is 4.27 MWh, which indicates an 8% reduction from STR to DTR scenario. Hence, the DTR applied in power lines has a greater impact on the reliability of IEHS for ensuring electric services. Moreover, the heating-service-based reliability of IEHS is slightly affected by DTR since some heating services depend on the reliable electric power supplies.

E. Case 5: Long-term Reliability Evaluation Results

Although the service-based reliability concerned in this paper is more related to the short-term timeframe, the long-term reliability evaluation is also worth studying. In this case, the one-year simulation is conducted using the proposed method, where the study period and time interval are 8760 hours and 1 hour, respectively. The scenario settings are consistent with the previous cases including Scenarios A and B. The tolerance level of variance coefficient is θ^{set} = 0.05.

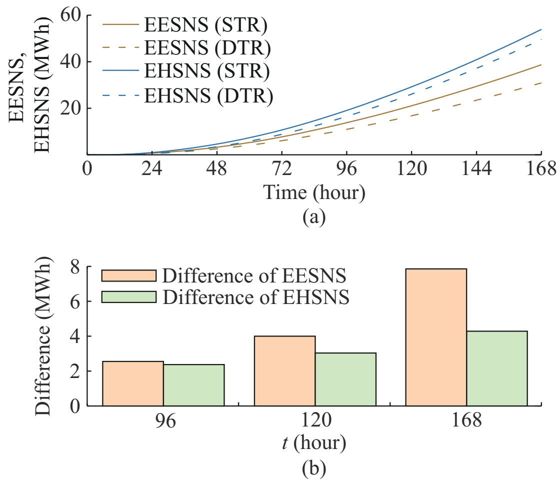

Fig. 12. Reliability indices EESNS and EHSNS and their differences in STR and DTR. (a) EESNS and EHSNS in STR and DTR scenarios. (b) Differences of reliability indices between STR and DTR scenarios.

The computation time of TSMCS for two scenarios is presented in Table IV. At the last iterations of two scenarios, the maximum coefficients of variance θ^t are 0.0490 and 0.0493. The two coefficients all satisfy the stopping criterion (36) and thus the simulations in two scenarios are converged. The long-term reliability results in different scenarios are presented in Table V. Similar to the one-week simulation results as presented before, the service-based reliability in Scenario B is improved compared with that in Scenario A due to the impacts of thermal dynamics. For example, the average LOHSP is reduced from 0.077 in Scenario A to 0.072 in Scenario B, because the amount of unacceptable IEHS states decreases when the dynamic services are considered. Besides, an 11.78% reduction can be observed in the average EHSNS from Scenario A to Scenario B, reaching 298.1 MWh. It indicates the decline of energy service losses during the one-year horizon, reflecting the cumulative benefits of thermal dynamics for the service-based reliability in the long term. Actually, the differences of reliability indices between the two scenarios would be more significant when the time interval of TSMCS is set to be a smaller value and the dynamic processes of energy can be better characterized. However, it is not applicable because a lot of computation time will be required to complete the long-term simulation with high temporal precision. This also shows that the service-based reliability evaluation technique for IEHS in this paper is more suitable for the operational phase with short-term timeframe, as previously analyzed in Section IV-B.

TABLE IV
Computation Time of TSMCS for Two Scenarios

Scenario	Number of iterations	Total time (hour)
A	3691	8.20
B	3974	9.41

TABLE V
Long-term Reliability Results in Different Scenarios

Scenario	LOESP	LOHSP	EESNS (MWh)	EHSNS (MWh)
A	0.092	0.077	1857.8	2532.2
B	0.088	0.072	2004.5	2830.3

VI. Conclusion

The service-based reliabilities of IEHSs from the perspective of customers are defined and analyzed in this paper, where thermal dynamics are considered to ensure the accuracy of the reliability analysis. The energy service performances of IEHSs in contingency states are firstly modelled. On this basis, the framework for service-based reliability analysis is further proposed. Besides, the pertinent reliability indices are proposed considering both the dynamic service performances and service satisfactions of customers.

The simulation results demonstrate that the proposed framework can effectively quantify the reliability levels of IEHSs based on energy services for customers. The reduced EESNS and EHSNS indicate that thermal dynamics can lessen the damage of IEHSs in contingency states. And the LOHSP can specifically represent the probability of the heating service loss by judging the acceptable or unacceptable states utilizing temperature-measured service performances. Moreover, both the thermal dynamic factors and the DTR could affect the reliability of IEHS, since they determine the potential energy storage capabilities of the system. During the long-term period, the service-based reliability of IEHS could benefit more from thermal dynamics due to the temporally cumulative effects. The reliability analysis results obtained from the proposed framework can provide the decision-making guidance for operators to ensure the reliable energy services for customers in IEHS.

References

[1] L. Chen, Q. Xu, Y. Yang *et al.*, "Community integrated energy system trading: a comprehensive review," *Journal of Modern Power Systems and Clean Energy*, vol. 10, no. 6, pp. 1445-1458, Nov. 2022.

[2] C. Yan, Z. Bie, S. Liu *et al.*, "A reliability model for integrated energy system considering multi-energy correlation," *Journal of Modern Power Systems and Clean Energy*, vol. 9, no. 4, pp. 811-825, Jul. 2021.

[3] X. Yin, C. Ye, Y. Ding *et al.*, "Exploiting internet data centers as energy prosumers in integrated electricity-heat system," *IEEE Transactions on Smart Grid*, vol. 14, no. 1, pp. 167-182, Jan. 2023.

[4] C. Shao, Y. Ding, P. Siano *et al.*, "A framework for incorporating demand response of smart buildings into the integrated heat and electricity energy system," *IEEE Transactions on Industrial Electronics*, vol. 66, no. 2, pp. 1465-1475, Feb. 2019.

[5] M. R. Haghifam and M. Manbachi, "Reliability and availability modelling of combined heat and power (CHP) systems," *International Journal of Electrical Power & Energy Systems*, vol. 33, pp. 385-393, Mar. 2011.

[6] X. Chen, C. Kang, M. O'Malley *et al.*, "Increasing the flexibility of combined heat and power for wind power integration in China: modeling and implications," *IEEE Transactions on Power Systems*, vol. 30, no. 4, pp. 1848-1857, Jul. 2015.

[7] H. Kim and C. Singh, "Reliability modeling and simulation in power systems with aging characteristics," *IEEE Transactions on Power Systems*, vol. 25, no. 1, pp. 21-28, Feb. 2010.

[8] X. Shan, P. Wang, and W. Lu, "The reliability and availability evaluation of repairable district heating networks under changeable external conditions," *Applied Energy*, vol. 203, pp. 686-695, Jul. 2017.

[9] C. Yan, Z. Bie, S. Liu *et al.*, "A reliability model for integrated energy

system considering multi-energy correlation," *Journal of Modern Power Systems and Clean Energy*, vol. 9, no. 4, pp. 811-825, Jul. 2021.

[10] L. Chi, H. Su, E. Zio *et al.*, "A systematic framework for the assessment of the reliability of energy supply in integrated energy systems based on a quasi-steady-state model," *Energy*, vol. 263, pp. 1-17, Jan. 2023.

[11] Y. Kou, Z. Bie, G. Li *et al.*, "Reliability evaluation of multi-agent integrated energy systems with fully distributed communication," *Energy*, vol. 224, pp. 1-14, Jun. 2021.

[12] Y. Ma, Y. Chi, D. Wu *et al.*, "Reliability of integrated electricity and gas supply system with performance substitution and sharing mechanisms," *Reliability Engineering & System Safety*, vol. 212, pp. 1-10, Aug. 2021.

[13] S. Wang, Y. Ding, C. Ye *et al.*, "Reliability evaluation of integrated electricity-gas system utilizing network equivalent and integrated optimal power flow techniques," *Journal of Modern Power Systems and Clean Energy*, vol. 7, no. 6, pp. 1523-1535, Nov. 2019.

[14] S. Zhang, M. Wen, H. Cheng *et al.*, "Reliability evaluation of electricity-heat integrated energy system with heat pump," *CSEE Journal of Power and Energy Systems*, vol. 4, pp. 425-433, Dec. 2018.

[15] J. Wang, C. Fu, K. Yang *et al.*, "Reliability and availability analysis of redundant BCHP (building cooling, heating and power) system," *Energy*, vol. 61, pp. 531-540, Nov. 2013.

[16] E. Bilgin, M. C. Caramanis, I. C. Paschalidis *et al.*, "Provision of regulation service by smart buildings," *IEEE Transactions on Smart Grid*, vol. 7, no. 3, pp. 1683-1693, May 2016.

[17] H. V. Larsen, H. Pálsson, B. Bøhm *et al.*, "Aggregated dynamic simulation model of district heating networks," *Energy Conversion and Management*, vol. 43, no. 8, pp. 995-1019, May 2002.

[18] M. Bao, Y. Ding, X. Yin *et al.*, "Definitions and reliability evaluation of multi-state systems considering state transition process and its application for gas systems," *Reliability Engineering & System Safety*, vol. 207, pp. 1-11, Dec. 2020.

[19] A. Benonysson, B. Bøhm, and H. F. Ravn, "Operational optimization in a district heating system," *Energy Conversion and Management*, vol. 36, no. 5, pp. 297-314, May 1995.

[20] H. Zhao, "Analysis, modelling, and operational optimization of district heating systems," Ph.D. dissertation, Centre for District Heating Technology, Technical University of Denmark, Lyngby, Denmark, 1995.

[21] T. Zhang, J. Wang, H. Zhong *et al.*, "Soft open point planning in renewable-dominated distribution grids with building thermal storage," *CSEE Journal of Power and Energy Systems*, vol. 9, no. 1, pp. 244-253, Jan. 2023.

[22] M. Tan, Y. Zhu, and J. Jin, "Study on dynamic reliability simulation analyzing method of thermodynamic process," in *Proceedings of 2012 International Conference on Quality, Reliability, Risk, Maintenance, and Safety Engineering*, Chengdu, China, Jun. 2012, pp. 258-262.

[23] I. Postnikov, "A reliability assessment of the heating from a hybrid energy source based on combined heat and power and wind power plants," *Reliability Engineering & System Safety*, vol. 221, pp. 1-13, May 2022.

[24] X. Shan, P. Wang, and W. Lu, "The reliability and availability evaluation of repairable district heating networks under changeable external conditions," *Applied Energy*, vol. 203, pp. 686-695, Oct. 2017.

[25] C. Cheng, Q. Sun, Y. Huang *et al.*, "Reliability evaluation of integrated energy system based on coupling equipment failure," in *Proceedings of 2020 Chinese Automation Congress (CAC)*, Shanghai, China, Nov. 2020, pp. 6566-6569.

[26] J. Lv, S. Zhang, H. Cheng *et al.*, "Reliability evaluation of integrated energy system considering the dynamic behaviour of loads and operation strategy," *Energy Procedia*, vol. 158, pp. 6508-6514, Feb. 2019.

[27] Y. Ding, C. Shao, B. Hu *et al.*, "Operational reliability assessment of integrated heat and electricity systems considering the load uncertainties," *IEEE Transactions on Smart Grid*, vol. 12, no. 5, pp. 3928-3939, Sept. 2021.

[28] J. Zeng, X. Wang, M. Cao *et al.*, "Reliability evaluation of coupled heat and electricity systems with CSP considering thermal dynamic characteristics," in *Proceedings of 2021 4th International Conference on Energy, Electrical and Power Engineering (CEEPE)*, Chongqing, China, Apr. 2021, pp. 12-18.

[29] G. Li, Y. Huang, and Z. Bie, "Reliability evaluation of smart distribution systems considering load rebound characteristics," *IEEE Transactions on Sustainable Energy*, vol. 9, no. 4, pp. 1713-1721, Oct. 2018.

[30] G. Li, Z. Bie, Y. Kou *et al.*, "Reliability evaluation of integrated energy systems based on smart agent communication," *Applied Energy*, vol. 167, pp. 397-406, Apr. 2016.

[31] B. Hu, Y. Sun, C. Shao *et al.*, "A decentralized market framework for procurement of operating reserves from district energy systems," *IEEE Transactions on Sustainable Energy*, vol. 12, no. 3, pp. 1629-1639, Jul. 2021.

[32] M. Cholette, H. Yu, P. Borghesani *et al.*, "Degradation modeling and condition-based maintenance of boiler heat exchangers using gamma processes," *Reliability Engineering & System Safety*, vol. 183, pp. 184-169, Mar. 2019.

[33] T. Guo, M. I. Henwood, and M. van Ooijen, "An algorithm for combined heat and power economic dispatch," *IEEE Transactions on Power Systems*, vol. 11, no. 4, pp. 1778-1784, Nov. 1996.

[34] W. M. Rohsenow, J. P. Hartnett, and E. N. Ganic, *Handbook of Heat Transfer Fundamentals*. New York: McGraw-Hill, 1985.

[35] J. Teh, C.-M. Lai, and Y.-H. Cheng, "Network topology optimisation based on dynamic thermal rating and battery storage systems for improved wind penetration and reliability," *IEEE Transactions on Reliability*, vol. 66, no. 4, pp. 1110-1119, Dec. 2017.

[36] J. Teh, C.-M. Lai, and Y.-H. Cheng, "Impact of the real-time thermal loading on the bulk electric system reliability," *IEEE Transactions on Reliability*, vol. 66, no. 4, pp. 1110-1119, Dec. 2017.

[37] C.-M. Lai and J. Teh, "Comprehensive review of the dynamic thermal rating system for sustainable electrical power systems," *Energy Reports*, vol. 8, pp. 3263-3288, Nov. 2022.

[38] J. Teh and C.-M. Lai, "Reliability impacts of the dynamic thermal rating and battery energy storage systems on wind-integrated power networks," *Sustainable Energy, Grids and Networks*, vol. 20, pp. 1-14, Dec. 2019.

[39] *IEEE Standard for Calculating the Current-temperature of Bare Overhead Conductors*, IEEE Std 738-2006, 2007.

[40] R. C. Sonderegger, "Dynamic models of house heating based on equivalent thermal parameters," Ph. D. dissertation, Princeton University, Princeton, USA, 1978.

[41] Q. Chen, R. Fu, and Y. Xu, "Electrical circuit analogy for heat transfer analysis and optimization in heat exchanger networks," *Applied Energy*, vol. 139, pp. 81-92, Feb. 2015.

[42] Y. Cao, W. Wei, L. Wu *et al.*, "Decentralized operation of interdependent power distribution network and district heating network: a market-driven approach," *IEEE Transactions on Smart Grid*, vol. 10, no. 5, pp. 5374-5385, Sept. 2019.

[43] Y. Ding, C. Singh, L. Goel *et al.*, "Short-term and medium-term reliability evaluation for power systems with high penetration of wind power," *IEEE Transactions on Sustainable Energy*, vol. 5, no. 3, pp. 896-906, Jul. 2014.

[44] A. Doucet, N. Freitas, and N. Gordon. (2001, Jan.). Sequential Monte Carlo methods in practice. [Online]. Available: https://link.springer.com/book/10.1007/978-1-4757-3437-9

[45] H. Yin, Z. Wang, Y. Liu *et al.*, "Operational reliability assessment of distribution network with energy storage systems," *IEEE Systems Journal*, vol. 17, no. 1, pp. 629-639, Mar. 2023.

[46] L. Cheng, X. Ye, J. He *et al.*, "Sequential short-term reliability evaluation considering repair time distribution," in *Proceedings of 2010 IEEE 11th International Conference on Probabilistic Methods Applied to Power Systems*, Singapore, Jun. 2010, pp. 178-183.

[47] H. Jia, Y. Ding, Y. Song *et al.*, "Operating reliability evaluation of power systems considering flexible reserve provider in demand side," *IEEE Transactions on Smart Grid*, vol. 10, no. 3, pp. 3452-3464, May 2019.

[48] O. Alsac and B. Stott, "Optimal load flow with steady-state security," *IEEE Transactions on Power Apparatus and Systems*, vol. PAS-93, no. 3, pp. 745-751, May 1974.

[49] X. Liu, J. Wu, N. Jenkins *et al.*, "Combined analysis of electricity and heat networks," *Applied Energy*, vol. 162, pp. 1238-1250, Jan. 2016.

Xunhu Yin received the B.S. degree in electrical engineering from Shandong University, Jinan, China, in 2019. He is currently pursuing the Ph.D. degree in electrical engineering from Zhejiang University, Hangzhou, China. His research interests include operation and optimization of the integrated energy system, reliability analysis, and regulation methods of flexible resources in smart grid.

Minglei Bao received the B.S. degree in electrical engineering from Shandong University, Jinan, China, and the Ph.D. degree in electrical engineering from Zhejiang University, Hangzhou, China, in 2016 and 2021, respectively. He is currently a postdoctor at Zhejiang University. His research interests include reliability analysis of integrated energy system, complex network, and power market.

Yi Ding received the bachelor's degree in electrical engineering from Shanghai Jiaotong University, Shanghai, China, in 2000, and the Ph. D. degree in electrical engineering from Nanyang Technological University, Singapore, in 2007. He is currently a Professor with the College of Electrical Engineering, Zhejiang University, Hangzhou, China. His research interests include power system reliability and performance analysis incorporating renewable energy resources, and reliability modeling and optimization of engineering systems.

Chengjin Ye received the B. E. and Ph. D. degrees in electrical engineering from Zhejiang University, Hangzhou, China, in 2010 and 2015, respectively. From 2015 to 2017, he served as a Distribution System Engineer with the Economics Institute, State Grid Zhejiang Electric Power Company Ltd., Hangzhou, China. From 2017 to 2019, he was an Assistant Research Fellow with the College of Electrical Engineering, Zhejiang University. Since 2020, he has been a Tenure-track Professor. His research interests include resilience enhancement of power grids and integrated energy systems, as well as market mechanism and control strategy towards the integration of demand resources into power system operation.

Peng Wang received the B.Sc. degree in electronic engineering from Xi'an Jiaotong University, Xi'an, China, in 1978, the first M. Sc. degree in electrical engineering from the Taiyuan University of Technology, Taiyuan, China, in 1987, and the second M. Sc. and Ph. D. degrees in electrical engineering from the University of Saskatchewan, Saskatoon, Canada, in 1995 and 1998, respectively. He is currently a Full Professor with the School of Electrical and Electronic Engineering, Nanyang Technological University, Singapore. His current research interests include power system planning and operation, renewable energy planning, solar or electricity conversion system, and power system reliability analysis.

Lalit Goel received the B.Tech. degree in electrical engineering from Regional Engineering College, Warangal, India, in 1983, and the M.Sc. and Ph.D. degrees in electrical engineering from the University of Saskatchewan, Saskatoon, Canada, in 1988 and 1991, respectively. In 1991, he joined the School of Electrical and Electronic Engineering, Nanyang Technological University, Singapore, where he is currently a Professor of power engineering and the Director of the Renaissance Engineering Program. His research interests include power system reliability analysis and power markets.